Sampled-grating DBR laser integrated with SOA and tandem electroabsorption modulator for chirp-control

L.A. Johansson, Y.A. Akulova, G.A. Fish and L.A. Coldren

Chirp-controlled optical modulation is demonstrated using a voltage division scheme applied to a long-section phase modulator to compensate for the positive chirp of an electroabsorption modulator arranged in a tandem configuration. Both modulators are integrated with a semiconductor optical amplifier (SOA) and a sampled-grating distributed Bragg reflector (DBR) laser. The effective chirp factor can be controlled from +1 to −0.86 with less than 2 dB penalty in extinction ratio and insertion loss.

Introduction: Widely tunable lasers integrated with electroabsorption modulators generally use a Franz-Keldysh modulator for wide spectral bandwidth [1]. The positive chirp of these modulators is a limiting factor for data transmission over long spans of fibre. Negative chirp and wide spectral bandwidth can be offered by integration of a widely tunable laser with a Mach-Zehnder modulator [2] at the cost of more complex modulator design and increased passive loss of the modulator. An alternative approach to generate negative chirp is using two EA modulators in a tandem configuration, one biased for amplitude modulation, the other biased for phase modulation using an inverted driver signal, compensating for the residual phase modulation of the amplitude modulator [3]. This approach is limited by the voltage swing available at the phase modulator, determined on the high voltage side by the diode threshold voltage, where carrier injection is causing distortion, and limited on the low voltage side by the onset of absorption that ultimately makes the insertion loss prohibitive and deteriorates the extinction ratio. One possibility to enhance the available performance of this approach is to use different bandgap EA modulators, possible to achieve using quantum-well intermixing techniques [4]. A second possibility that applies to Franz-Keldysh modulators is to use a simple voltage division scheme, which is described in this Letter.

Device design: Fig. 1 shows a schematic diagram of the device used in this work together with the voltage division scheme used. The electroabsorption modulator is split in two parts arranged in a tandem configuration. The device is mounted onto an aluminium nitride RF carrier, with integrated thin-film resistors. The amplitude modulator is terminated in parallel to 50 Ω in series with a capacitor. In contrast, the phase modulator is terminated in parallel by a lower value resistor and in series by a second resistor, such that $R_1 + R_2 = 50\ \Omega$. The resulting voltage division factor, n, is given by $n = 50\ \Omega/R_1$. To compensate for the lower modulation voltage, the phase modulator is made n times longer than the amplitude modulator. To a first-order estimate, the *RC*-limited bandwidth of the modulators remains the same. The main advantage of the described voltage division scheme is that while the modulation voltage is now scaled down by a factor of n, the threshold voltage stays constant, increasing the available phase swing while keeping amplitude modulation in the phase modulator low.

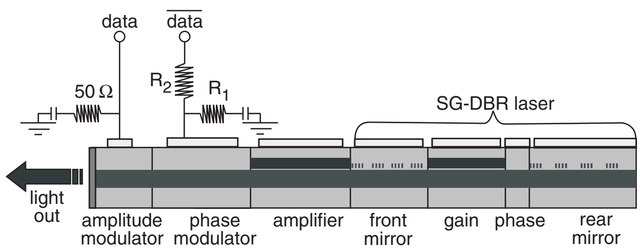

Fig. 1 *Schematic diagram of tandem EAM modulator, integrated with SOA and sampled-grating DBR laser; simple schematic of voltage division scheme also shown*

Two devices are investigated, the first having a 200 μm amplitude modulator and an 800 μm phase modulator, with a voltage division factor of $n = 4$. The second device has equal length sections of 120 μm, and is used for verification of the benefits of the principle. The sampled-grating DBR lasers are similar to the one described in [2], with more than 10 mW output power, lower than 2 MHz linewidth, and more than 40 dB side-mode suppression ratio, achieved over more than 40 nm wavelength tuning range.

Experimental results: The amplitude modulator is modulated at 2.5 Gbit/s datastream while the phase modulator is complementary modulated by the inverted signal. By varying the attenuation/amplification of the signal applied to the phase modulator, the resulting chirp of the device can be controlled. The time-resolved chirp characteristics of the modulated optical signal is measured using an Advantest Q7606B optical chirp form test set and an Agilent 86100A oscilloscope. The effective chirp factor, α_{eff}, is then derived from the time-resolved chirp data. Previously, using the amplitude modulator only, the effective chirp parameter has been shown to correlate well to the fibre dispersion penalty for this type of device [5].

Fig. 2 shows the measured chirp forms for the device when voltage division of $n = 4$ was used. The phase modulator was biased at 0 V and the amplitude modulator at −2.6 V. The upper plot shows the chirp characteristics of the amplitude modulator alone, corresponding to an α_{eff} of 0.97. Applying a modulation signal to the phase modulator of equal amplitude as to the amplitude modulator, results in the characteristics shown by the centre plot, corresponding to α_{eff} of 0.03. The remaining frequency chirping, particularly apparent at the falling edge, is a result of different impulse response between the phase and amplitude modulator. The different impulse response can be attributed in part to the inductance of the bondwire used to connect the modulators to the RF lines of the carrier. A more careful RF design should further decrease the envelope of the frequency chirp. The lower plot in Fig. 2 shows α_{eff} of −0.86 for a phase modulation signal amplified by 3 dB relative to that of the amplitude modulator.

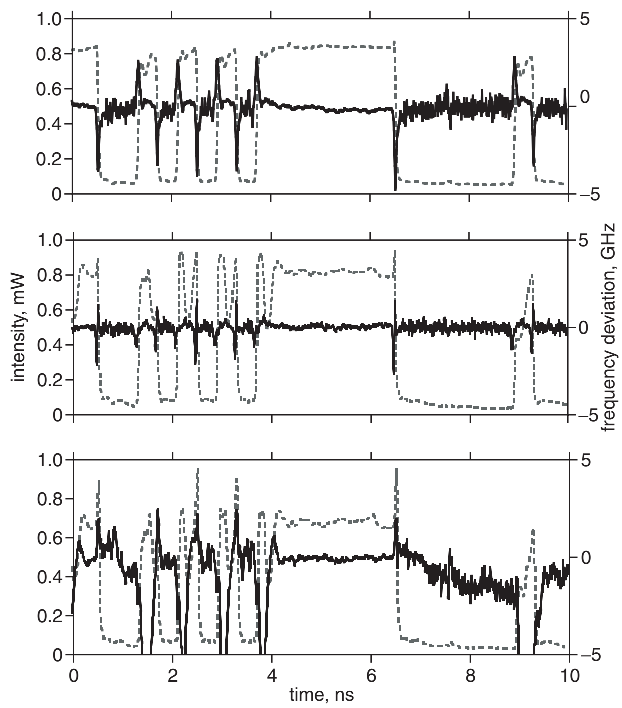

Fig. 2 *Measured output amplitude (dotted line) and time-resolved frequency chirping (solid line) of tandem EAM configuration*

Resulting effective chirp factors 0.97, 0.03, −0.86, respectively, top to bottom

Fig. 3 shows the extinction and excess insertion loss compared to amplitude modulation only against achieved effective chirp factor for a device using voltage division and a control device with equal length modulators. Significant penalties are shown for the control device at lower chirp values, as a result of counteracting amplitude modulation in the phase modulator. Using voltage division, α_{eff} down to −0.86 is observed with <2 dB excess insertion loss and <2 dB degradation of extinction ratio. For even lower values of achieved effective chirp, further degradation is observed, partly due to too high applied voltage in the phase modulator. This can be traded-off with a slightly degraded insertion loss and extinction by lowering the bias point of the phase modulator.

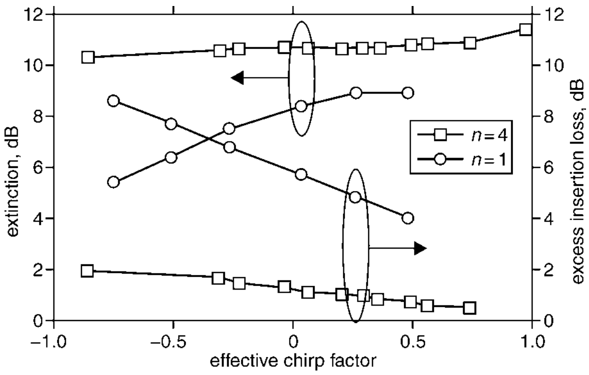

Fig. 3 *Extinction ratio and resulting penalty in terms of insertion loss, compared to amplitude modulation only, against measured large-signal chirp factor for n = 4 and n = 1*

The control device achieves negative chirp with lower phase modulation voltage. The cause for this is believed to be localised heating at the front edge of the phase modulator that for the control device experiences significant optical absorption, with the higher applied modulation voltage and therefore necessarily lower bias point: −2 V.

Conclusion: We have demonstrated how two Franz-Keldysh modulators arranged in a tandem configuration can be used to produce chirp-controlled optical modulation with an effective chirp factor down to −0.86. It is shown how using a long phase modulating section in combination with a simple voltage division scheme to one of the modulator sections can improve the performance of the tandem modulator to <2 dB excess insertion loss and <2 dB degradation of extinction ratio compared to a single section modulator for effective chirp factors down to −0.86.

24 October 2003

Electronics Letters online no: 20040016
doi: 10.1049/el:20040016

L.A. Johansson and L.A. Coldren (*Department of Electrical and Computer Engineering, University of California, Santa Barbara, CA 93106, USA*)

E-mail: leif@ece.ucsb.edu

Y.A. Akulova and G.A. Fish (*Agility Communications, Inc., 600 Pine Ave, Santa Barbara, CA 93117, USA*)

References

1 Akulova, Y.A., *et al.*: 'Widely-tunable electroabsorption-modulated sampled grating DBR laser transmitter', *IEEE J. Sel. Top. Quantum Electron.*, 2002, **8**, pp. 1349–1357

2 Barton, J.S., *et al.*: 'Widely-tunable high-speed transmitters using integrated SGDBRs and Mach-Zehnder modulators', *IEEE J. Sel. Top. Quantum Electron.* (accepted for publication)

3 Claassen, M., Harth, W., and Stegmüller, B.: 'Two-section electroabsorption modulator with negative chirp at low insertion loss', *Electron Lett.*, 1996, **32**, pp. 2121–2122

4 Skogen, E.J., *et al.*: 'A quantum-well-intermixing process for wavelength-agile photonic integrated circuits', *IEEE J. Sel. Top. Quantum Electron.*, 2002, **8**, pp. 863–869

5 Koh, P.C., *et al.*: 'Correlation between dispersion penalty and time-resolved chirp for widely tunable electroabsorption-modulated SGDBR laser across the EDFA gain bandwidth', *IEEE Photonics Technol. Lett.*, 2003, **15**, pp. 1011–1013